

## Supplementary Material

### Scalable fabrication of inch-sized FAPbI<sub>3</sub> perovskite wafers for highly sensitive near-infrared photodetection

Chao Li<sup>#</sup>, Zuolin Zhang<sup>#</sup>, Chenglin Wang, Mengjia Li, Jike Ding, Cong Chen\*

State Key Laboratory of Reliability and Intelligence of Electrical Equipment, School of Materials Science and Engineering, Hebei University of Technology, Tianjin 300401, China.

<sup>#</sup>Authors contributed equally.

**Correspondence to:** Prof. Cong Chen, State Key Laboratory of Reliability and Intelligence of Electrical Equipment, School of Materials Science and Engineering, Hebei University of Technology, No. 5340, Xiping Road, Beichen District, Tianjin 300401, China. E-mail: chencong@hebut.edu.cn

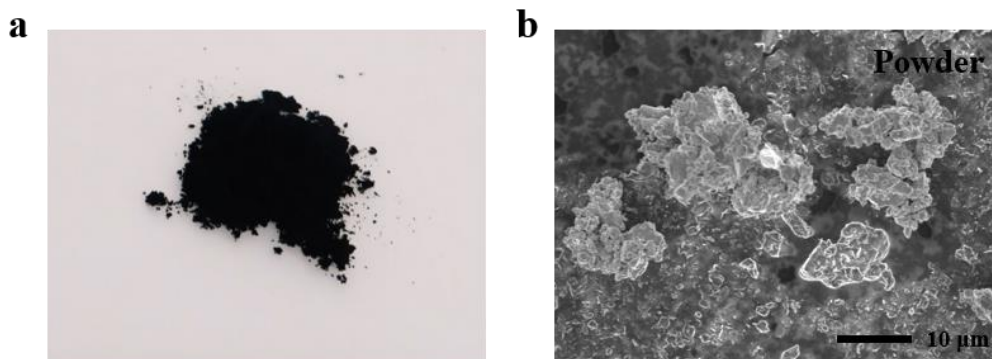


**Fig. S1** (a) Photo and (b) SEM of FAPbI<sub>3</sub> powder.



**Fig. S2** Photos of hot-press device.

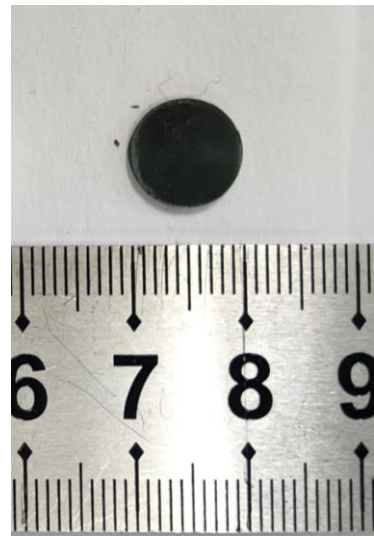


**Fig. S3** Photos of wafer with a diameter of 1 cm.

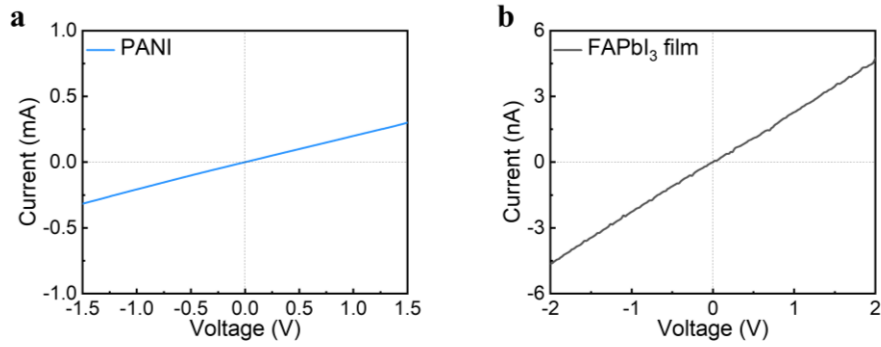


**Fig. S4** The  $J$ - $V$  curves of (a) PANI and (b) FAPbI<sub>3</sub> film.

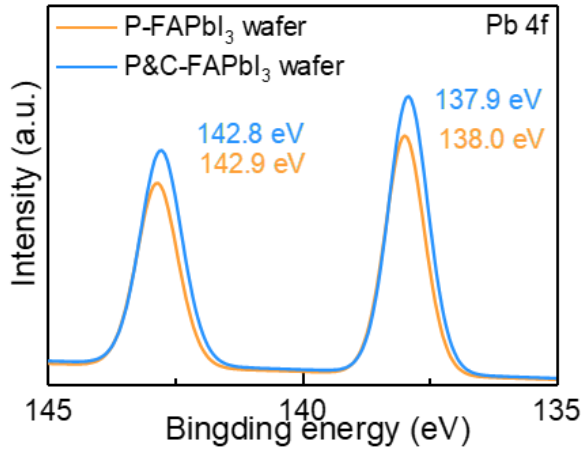


**Fig. S5** Pb 4f XPS spectra of P-FAPbI<sub>3</sub> wafer and P&C-FAPbI<sub>3</sub> wafer.

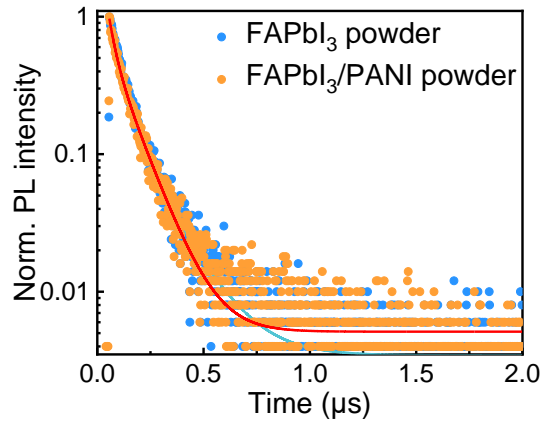


**Fig. S6** TRPL spectra of FAPbI<sub>3</sub> and FAPbI<sub>3</sub>/PANI powder.

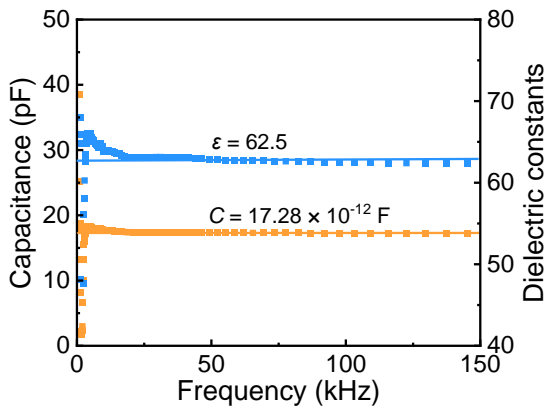


**Fig. S7** Frequency-dependent electrical curves of P&C-FAPbI<sub>3</sub> wafer detector.

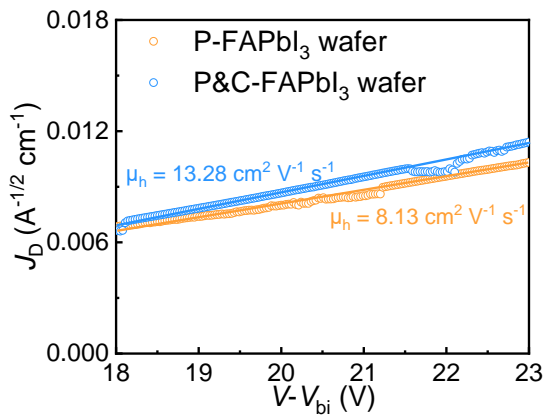


**Fig. S8** Hole mobility of the wafer detectors with or without PANI modification.

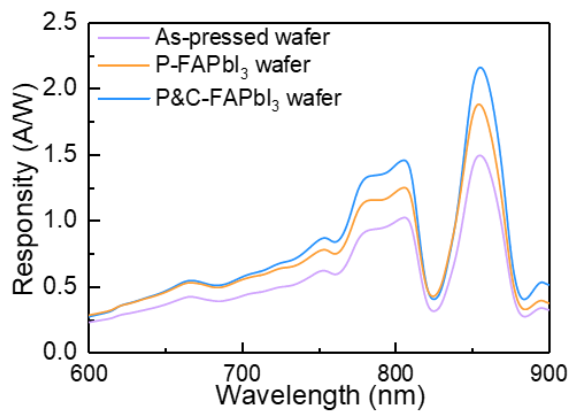


**Fig. S9** Responsivity of the photodetectors.

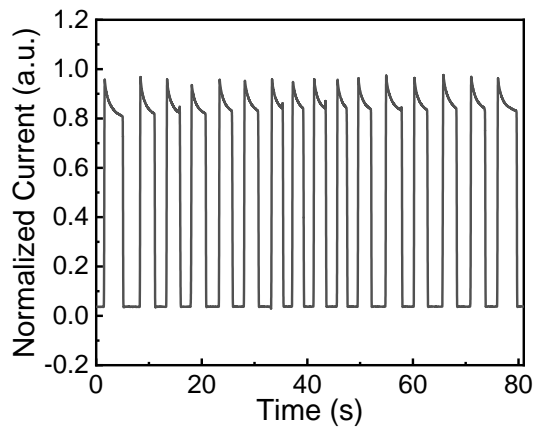


**Fig. S10** The photocurrent response curves of the P&C-FAPbI<sub>3</sub> wafer detector under an 520 nm light source at 5 V bias.

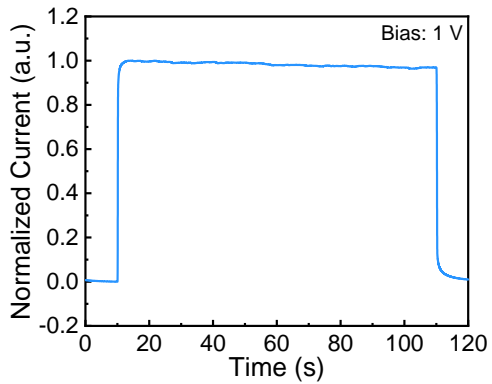


**Fig. S11** Operational stability of the P&C-FAPbI<sub>3</sub> wafer photodetector under an 845 nm wavelength at 1 V bias.

**Table S1** Physical properties of all chemicals such as FAPbI<sub>3</sub> and PANI.

Samples	Melting point	Density	Solubility
FAPbI <sub>3</sub> powder	387 °C	4.32 g/cm <sup>3</sup>	
Polyaniline (PANI)	>330 °C	1.36 g/mL	Soluble in polar solvents

**Table S2** Fitting data of TRPL curve in Figure 2h based on double exponential function.

Samples	$\tau_1$ (μs)	$A_1$	$\tau_2$ (μs)	$A_2$	$\tau_{ave}$ (μs)
As-pressed wafer	0.71	0.94	3.31	0.06	1.34
P-FAPbI <sub>3</sub> wafer	1.02	0.95	5.11	0.05	1.86
P&C-FAPbI <sub>3</sub> wafer	1.64	0.87	6.74	0.13	3.62

**Table S3** Response time of different type photodetectors.

Materials	Crystal	$\tau_{rise}$	$\tau_{fall}$	Reference
MAPbI <sub>3</sub>	Film	~10 ms	~10 ms	<sup>1</sup>
MAPbI <sub>3</sub>	Film	12.7 ms	6.9 ms	<sup>2</sup>
FAPbI <sub>3</sub>	Film	13 ms	11 ms	<sup>3</sup>
MAPb(Br <sub>0.78</sub> I <sub>0.22</sub> ) <sub>3</sub>	Single crystal	3.4 ms	3.6 ms	<sup>4</sup>
FAPbI <sub>3</sub>	Single crystal	17 ms	21 ms	<sup>5</sup>
FAPbI <sub>3</sub>	Single crystal	8.3 ms	7.5 ms	<sup>6</sup>
FAPbI <sub>3</sub>	Single crystal	214 μs	227 μs	<sup>7</sup>
FAPbI <sub>3</sub>	Wafer	810 μs	6.1 ms	This work

## Reference

1. Wu, H.; Su, Z.; Jin, F.; Zhao, H.; Li, W.; Chu, B. Improved performance of perovskite photodetectors based on a solution-processed  $\text{CH}_3\text{NH}_3\text{PbI}_3/\text{SnO}_2$  heterojunction. *Org. Electron.* **2018**, *57*, 206-210. DOI: 10.1016/j.orgel.2018.03.018.
2. Wang, J.; Xiao, S.; Qian, W.; Zhang, K.; Yu, J.; Xu, X.; Wang, G.; Zheng, S.; Yang, S. Self-Driven Perovskite Narrowband Photodetectors with Tunable Spectral Responses. *Adv. Mater.* **2021**, *33* (3), e2005557. DOI: 10.1002/adma.202005557.
3. Wang, C.; Zhang, Z.; Zhao, X.; Zhu, Y.; Li, M.; Ding, J.; Chen, C. An interdiffusion-controlled nucleation strategy for efficient sequential deposition of perovskite photovoltaics. *Mater. Chem. Front.* **2023**, *7* (19), 4497-4507.
4. Zhang, Y.; Liu, Y.; Li, Y.; Yang, Z.; Liu, S. F. Perovskite  $\text{CH}_3\text{NH}_3\text{Pb}(\text{Br}_{x}\text{I}_{1-x})_3$  single crystals with controlled composition for fine-tuned bandgap towards optimized optoelectronic applications. *J. Mater. Chem. C* **2016**, *4* (39), 9172-9178.
5. Han, Q.; Bae, S. H.; Sun, P.; Hsieh, Y. T.; Yang, Y. M.; Rim, Y. S.; Zhao, H.; Chen, Q.; Shi, W.; Li, G.; et al. Single crystal formamidinium lead iodide ( $\text{FAPbI}_3$ ): insight into the structural, optical, and electrical properties. *Adv. Mater.* **2016**, *28* (11), 2253-2258. DOI: 10.1002/adma.201505002.
6. Liu, Y.; Sun, J.; Yang, Z.; Yang, D.; Ren, X.; Xu, H.; Yang, Z.; Liu, S. F. 20-mm-Large Single-Crystalline Formamidinium-Perovskite Wafer for Mass Production of Integrated Photodetectors. *Adv. Opt. Mater.* **2016**, *4* (11), 1829-1837. DOI: 10.1002/adom.201600327.
7. Chu, D.; Jia, B.; Liu, N.; Zhang, Y.; Li, X.; Feng, J.; Pi, J.; Yang, Z.; Zhao, G.; Liu, Y.; et al. Lattice engineering for stabilized black  $\text{FAPbI}_3$  perovskite single crystals for high-resolution x-ray imaging at the lowest dose. *Sci. Adv.* **2023**, *9* (35), eadh2255. DOI: doi:10.1126/sciadv.adh2255.